JACS
JOURNAL OF THE AMERICAN CHEMICAL SOCIETY

COMMUNICATION

pubs.acs.org/JACS

Chiral Sum Frequency Generation Spectroscopy for Characterizing Protein Secondary Structures at Interfaces

Li Fu, Jian Liu, and Elsa C. Y. Yan*

Department of Chemistry, Yale University, 225 Prospect Street, New Haven, Connecticut 06520, United States

Supporting Information

ABSTRACT: *In situ* and real-time characterization of protein secondary structures at interfaces is important in biological and bioengineering sciences, yet remains technically challenging. In this study, we used chiral sum frequency generation (SFG) spectroscopy to establish a set of vibrational optical markers for characterizing protein secondary structures at interfaces. We discovered that the N−H stretches along the peptide backbones of α-helices can be detected in chiral SFG spectra. We further observed that the chiral vibrational signatures of the N−H stretch together with the peptide amide I are unique to α-helix, β-sheet, and random coil at interfaces. Using these chiral vibrational signatures, we studied the aggregation of human islet amyloid polypeptide (hIAPP), which is implicated in type II diabetes. We observed *in situ* and in real time the misfolding of hIAPP from random coils to α-helices and then β-sheets upon interaction with a lipid−water interface. Our findings show that chiral SFG spectroscopy is a powerful tool to follow changes in protein conformations at interfaces and identify interfacial protein secondary structures that elude conventional techniques.

In situ and real time characterization of protein secondary structures at interfaces is important for understanding the biological function of proteins and developing biomaterials and biosensors. However, the lack of surface-sensitive and label-free techniques that can unambiguously differentiate secondary structures at interfaces poses challenges. Consequently, problems that require identification of secondary structures at the interfaces of complex protein systems have not been fully explored. For example, the aggregation of amyloid proteins into β-sheet structures is associated with many diseases, such as Parkinson's, Alzheimer's, and prion diseases.[1] Although recent findings reveal the importance of lipid membranes in catalyzing the aggregation process,[2,3] the aggregation pathway of amyloid proteins on membrane surfaces is not fully understood.

Here, we introduced a concept of using second-order chiral vibrational optical markers, provided by sum frequency generation (SFG) spectroscopy, to distinguish protein secondary structures at interfaces. We studied chiral vibrational structures of peptide backbones and observed characteristic N−H stretch and amide I signatures that are unique to random coils, α-helices, and β-sheets at interfaces. Using these signatures, we monitored the aggregation of human amyloid polypeptide (hIAPP) at a lipid−water interface and observed the conversion of hIAPP from a random coil to an α-helix and then to a β-sheet in real time. We found that the optical markers are free from background of solvents and achiral solutes at the interfaces. They are in the spectral regions of the amide I and N−H stretch widely separated at 1600−1700 cm^{-1} and 3100−3350 cm^{-1}, respectively. Hence, the SFG vibrational markers are relatively optically clean and background-free. Thus, they are useful for characterizing interfacial protein secondary structures that have been difficult to resolve using conventional techniques.

Conventional techniques for characterizing protein secondary structures at interfaces have limitations. Although circular dichroism (CD) is often used to characterize secondary structures,[4] it lacks surface sensitivity. Surface plasmon resonance can detect adsorption of proteins on surfaces,[5] but it is not sensitive to secondary structures. The X-ray scattering method can be used to probe the ordered protein structures, but it is not suited for kinetic studies *in situ*. Raman and infrared (IR) spectroscopy can provide information about secondary structure by probing amide I vibrational bands.[6−9] However, amide I vibrational bands overlap with the bending modes of water. Thus, deuterated water must be used. Moreover, the amide I bands of various secondary structures are clustered in the spectral region of 1620−1680 cm^{-1} and the amide I bands of α-helices and random coils are both approximately at 1650 cm^{-1}, which makes characterization of complex protein systems extremely difficult. Both Raman and IR spectroscopy lack surface selectivity and often require metal substrates to enhance surface signal[5,10] or reflection geometry to suppress bulk signals.[11] Two-dimensional IR spectroscopy has been used to identify secondary structures.[12−15] However, it can only be applied to proteins in bulk solution, not at interfaces.

Since the late 1980s, SFG spectroscopy has been developed into a powerful surface-selective technique to obtain structural and dynamic information in physical and material sciences,[16−20] such as probing chemical physics of small molecules at interfaces.[21−25] It is a second-order coherent optical technique, requiring spatial and temporal overlap of an IR beam and a visible beam at the interface, to produce vibrational optical signals. SFG is surface-selective due to the intrinsic asymmetry of the interface such that second-order polarization induced at interfacial molecules can add up coherently to produce surface selective signals.[16] Simpson et al. derived a chiral SFG theory to show that signals can be generated even from achiral molecules that are arranged in macromolecular chiral architectures.[26] Such signals

Received: February 19, 2011
Published: May 02, 2011

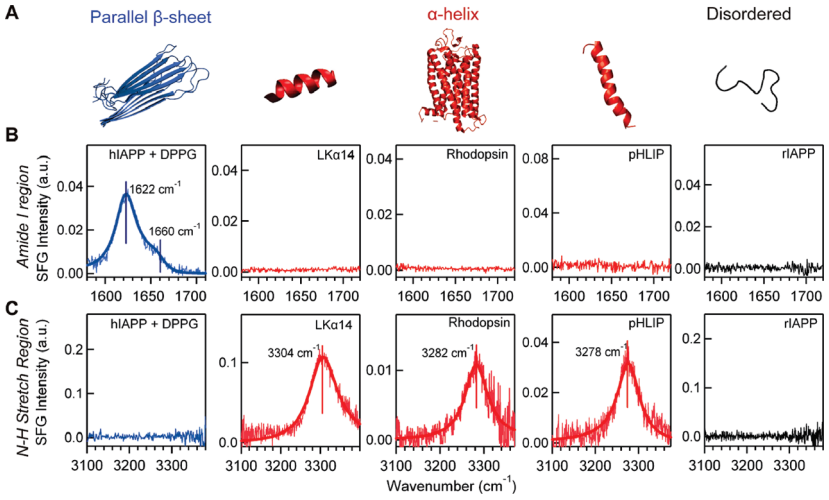

Figure 1. Chiral SFG spectra of the model peptides and protein. (A) Schematics of secondary structures of the hIAPP aggregate, $LK_{\alpha}14$, rhodopsin, pHLIP, and rIAPP. The chiral SFG spectra at the air−water interface in the (B) amide I region and (C) N−H stretch region.

have been observed experimentally using biomolecules, including the C−H stretches of DNA and the amide I of proteins.[27−30] Inspired by the chiral SFG theory and detection of the chiral amide I signal from β-sheets,[28,30] we realized that the N−H groups along chiral peptide backbones of various secondary structures could also be chiral-SFG active. To test this idea, we probed both the N−H stretch and amide I regions of model peptides and proteins. We observed that chiral N−H stretch and amide I are highly unique to the α-helix and the β-sheet. We propose using these signals as optical markers to characterize protein secondary structures at interfaces, similar to the use of CD signals to identify protein secondary structures in bulk solution.

To establish the chiral vibrational optical markers, we obtained the SFG spectra of model peptides and proteins (Figure 1A). For β-sheets, we used hIAPP, a 37-amino acid peptide hormone secreted by human pancreatic β-cells. This peptide forms parallel β-sheets at the air−water interface in the presence of negatively charged lipids.[31] For α-helices, we chose three model systems: (1) $LK_{\alpha}14$, a 14-amino acid peptide with the sequence $(LKKLLKL)_2$;[32] (2) pH-low insertion peptide (pHLIP), a 36-amino acid peptide derived from helix 3 of bacteriorhodopsin;[33] and (3) bovine rhodopsin, a 7-α-helical transmembrane G protein-coupled receptor.[34] A combination of techniques, including CD spectroscopy, IR spectroscopy, and X-ray photoelectron spectroscopy, has shown that $LK_{\alpha}14$ and pHLIP can form α-helices in amphiphilic environments.[32,33,35,36] Rhodopsin can form a stable monolayer at the air−water interface when surface pressure is carefully controlled in a Langmuir trough.[37,38] As a control, we used rat islet amyloid polypeptide (rIAPP), which differs from hIAPP by six amino acids.[39] It is relatively unstructured in solution and does not form β-sheet structures even in the presence of lipids.[3]

To obtain the SFG spectra, we dissolved the peptides in aqueous solution and probed them at the air−water interface (Supporting Information). For the hIAPP experiments, we added lipid molecules to induce the formation of amyloid at the air−water interface. For the rhodopsin experiments, we expressed and purified recombinant bovine rhodopsin[40] and made a monolayer of rhodopsin at the air−water interface, as described by Lavoie et al.[38] We used our broad-bandwidth SFG spectrometer[41] to obtain the chiral and achiral SFG spectrum of each peptide and protein in both the N−H stretch and amide I regions. We used *psp* (*p*-polarized SFG, *s*-polarized visible, and *p*-polarized infrared) polarization for the acquisition of chiral SFG spectra (Figure 1) and *ssp* polarization for the acquisition of achiral spectra (Figure S1).

In the presence of the negatively charged lipid dipalmitoylphosphoglycerol (DPPG), hIAPP aggregates into a parallel β-sheet structure at the air−water interface. The hIAPP aggregate shows a peak at 1622 cm^{-1} and a shoulder at 1660 cm^{-1} in the amide I chiral spectrum, corresponding to the antisymmetric and symmetric amide I modes, respectively (Figure 1),[30,42] but it does not show a signal in the chiral N−H spectrum. In contrast, α-helical rhodopsin and pHLIP show chiral N−H signals at about 3280 cm^{-1} and $LK_{\alpha}14$ shows a chiral N−H signal at about 3300 cm^{-1}. However, all are silent in the amide I chiral spectra (Figure 1). Conversely, the achiral SFG spectrum of every peptide or protein, obtained using *ssp* polarization (Figure S1), shows both amide I and N−H stretch signals regardless of their secondary structures. Similar to conventional IR and Raman spectroscopy, achiral SFG spectroscopy does not allow direct identification of secondary structures. Moreover, the rIAPP control shows an achiral signal in the amide I spectrum (Figure S1), indicating that rIAPP adsorbs at the interface. However, we could not detect a chiral N−H stretch or amide I signal (Figure 1), suggesting that not every protein or peptide at interfaces can generate a chiral N−H or amide I signal under our experimental conditions. It is likely that rIAPP adopts a largely disordered structure or a partially folded structure[43], which does not generate detectable chiral signals. Our results indicate that parallel β-sheets exhibit chiral amide I signals but are silent in the chiral N−H stretch spectrum, whereas α-helices display chiral N−H stretch signals but are silent in the chiral amide I spectrum. Because random coils do not have a chiral peptide backbone, they should not show a chiral N−H or amide I signal at the interface. Taken together, these results identify a set of chiral vibrational SFG optical markers that can be used to characterize protein secondary structures at interfaces.

To demonstrate the use of these optical markers, we studied hIAPP as a model system, which aggregates into β-sheet-rich structures[44,45] deposited onto pancreatic β-cells and causes type II diabetes.[46] The aggregation of hIAPP is catalyzed by interactions with negatively charged lipids[2,3] and is thought to undergo an α-helical intermediate before aggregating into β-sheet structures,

dx.doi.org/10.1021/ja201575e | *J. Am. Chem. Soc.* 2011, 133, 8094–8097

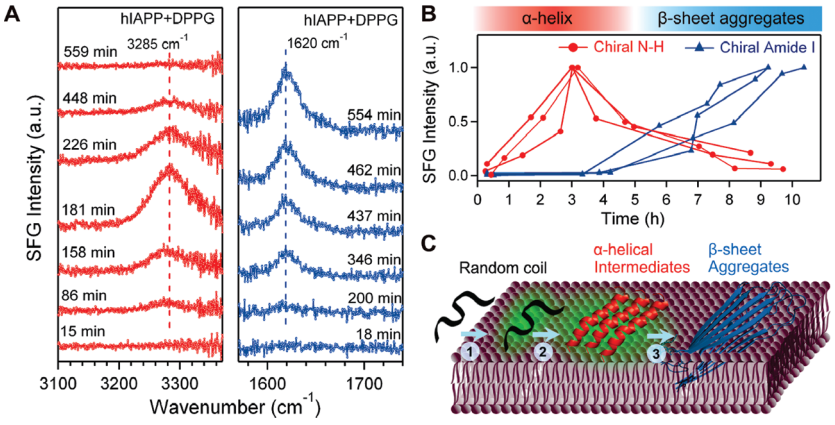

Figure 2. Aggregation of hIAPP. (A) The time-dependent chiral SFG spectra in the vibrational regions of N−H stretch (left) and amide I (right) after addition of DPPG. (B) The intensity of the N−H stretch and amide I signals as a function of time. Results of triplicate experiments are shown. (C) The aggregation model of hIAPP on a membrane surface as observed in the SFG experiments: adsorption as a random coil leads to formation of α-helical intermediates, which are converted to β-sheet aggregates.

based on extensive biophysical studies using a combination of techniques, including CD, fluorescence, and IR reflection absorption spectroscopy.[31,47]

Following addition of DPPG, we monitored chiral SFG spectra of hIAPP in the N−H stretch and amide I spectral regions at the air−water interface (Figure 2A). The signal of the N−H stretch gradually increases to its maximum in 3 h and disappears by 10 h after the addition of DPPG. In contrast, the amide I signal appears approximately 4 h after addition of DPPG and reaches its maximum in 10 h. Because the kinetics of amyloid formation is difficult to reproduce due to variations in factors such as nucleation and agitation,[48] we repeated each measurement three times and plotted the N−H stretch and amide I intensity as a function of time (Figure 2B). Our findings show that the N−H stretch signal consistently disappeared prior to accumulation of the amide I signal. As control experiments, we studied hIAPP in the absence of DPPG (Figure S2A−B) and rIAPP in the presence of DPPG (Figure S2C−D) because neither peptide aggregates into a β-sheet under these conditions in the time scale of hours.[1,30] In both experiments, we observed the achiral amide I signals, suggesting both peptides adsorb at the interface.[30] However, monitoring the N−H and amide I chiral spectra for approximately 10 h, we could not detect any chiral signal (Figure S2). Our results indicate that neither hIAPP nor rIAPP forms a β-sheet and that neither hIAPP nor rIAPP folds into an α-helical structure that can be detected in our experiments.

On the basis of the N−H signal at 3285 cm^{-1}, which corresponds to an α-helix, and the amide I signal at 1620 cm^{-1}, which corresponds to a parallel β-sheet, the results presented in Figure 2 show a transient α-helical intermediate and a final parallel-β-sheet product in the amyloid aggregation process. The initial absence of an amide I signal could mean that hIAPP begins in either an α-helical or a random-coil structure. However, the initial absence of the N−H stretch signal reveals that hIAPP is a random coil. Due to spectral overlap in the amide I region, it is difficult to distinguish random coils and α-helices using IR and Raman spectroscopy. We conclude that hIAPP adsorbs at the lipid−water interface as a random coil and begins folding into an α-helix within 1−1.5 h. It converts fully to an α-helix at approximately 3 h and folds into parallel β-sheets at approximately 9 h. Given these findings, we can use the SFG optical markers to explicitly identify the α-helical intermediate and follow the kinetics of changes in the secondary structure of hIAPP at the lipid−water interface.

Interestingly, the amide I and N−H stretch behave differently in the chiral SFG spectra. At present, a quantitative description of the chiral N−H and amide I signals from α-helices and β-sheets is being developed. Our observed chiral amide I response is in qualitative agreement with the theory developed by Perry et al.,[49] which predicts a larger contribution of the chiral amide I response from β-sheets and a smaller contribution from α-helices. The observed differences in the chiral SFG signals may be originated from the symmetry of the vibrational modes and the coupling of the vibrational modes in the peptide backbones. It is known that individual N−H stretches are highly localized,[50] while individual amide I modes are strongly coupled in the peptide backbones.[9] We speculate that the vibrational coupling can play a role in the SFG chiral-optical response.

Moreover, we argue that the chiral SFG signals that we observed originate from the interfaces due to the chiral macromolecular arrangement of the peptide backbones.[26] Although the SFG chiral-optical response could be observed from the bulk of chiral liquid,[51] this bulk chiral signal is due to the asymmetry of the Raman tensor, which is very weak and needs the visible beam to be in resonance with the electronic transition of the molecules. In addition, this bulk chiral signal was detected by the transmission optical geometry from the bulk of pure chiral liquid as reported previously.[51] In contrast, the chiral SFG signal observed in our experiment is comparable to the achiral signals, and these relatively strong chiral signals were detected at low concentration (1−5 μM) using reflective geometry without electronic resonance. Hence, it is not likely that our observed chiral SFG signals are from the bulk.

Overall, our results show the advantages of using chiral SFG to probe interfacial protein structures. First, the chiral SFG vibrational signatures are optically clean. The amide I signal from a β-sheet and the N−H signal from an α-helix do not interfere with each other. The chiral SFG signal is also insensitive to the presence of achiral solvents and achiral solutes at interfaces. Hence, the SFG markers are optically clean and relatively background-free. Second, kinetic information can be readily obtained by monitoring the SFG optical signals, which enables kinetic studies of protein folding and misfolding at interfaces and

dx.doi.org/10.1021/ja201575e |J. Am. Chem. Soc. 2011, 133, 8094–8097

surface characterizations of biomaterials and biosensors, without the use of spectroscopic labels. Because SFG is surface-selective, only a monolayer of protein in the amount of micrograms is needed to obtain SFG spectra. This small sample size allows the study of most proteins that can be purified from natural sources or recombinant expression systems, including membrane proteins, which are difficult to obtain. Moreover, SFG can be used to measure the orientation of secondary structures at interfaces,[52] and thus can be used to study biological processes, which often involve subtle conformational changes in proteins. Furthermore, SFG can be used to probe distinct vibrational structures of individual side chains and other biomolecules, allowing studies of highly specific protein interactions at interfaces. Finally, as SFG uses ultrafast lasers, which provide nanosecond to femtosecond time resolution, it enables studies of ultrafast vibrational dynamics of proteins. For all these reasons, chiral SFG spectroscopy is expected to be useful for solving a variety of problems related to structures, functions, and dynamics of proteins at interfaces that conventional techniques cannot adequately address.

■ ASSOCIATED CONTENT

Supporting Information. Materials, SFG Setup, Experimental Procedure and Data Acquisition, Figures S1 and S2. This material is available free of charge via the Internet at http://pubs.acs.org.

■ AUTHOR INFORMATION

Corresponding Author
elsa.yan@yale.edu

■ ACKNOWLEDGMENT

The authors thank Dr. R. Tykco for providing the structure of the parallel β-sheet aggregates of hIAPP. E.Y. is the recipient of the Starter Grant Award, Spectroscopy Society of Pittsburgh. J.L. is an Anderson Postdoctoral fellow. The authors thank Dr. S. G. Ray for helpful discussions.

■ REFERENCES

(1) Chiti, F.; Dobson, C. M. *Annu. Rev. Biochem.* **2006**, *75*, 333–366.
(2) Jayasinghe, S. A.; Langen, R. *Biochemistry* **2005**, *44*, 12113–12119.
(3) Knight, J. D.; Hebda, J. A.; Miranker, A. D. *Biochemistry* **2006**, *45*, 9496–9508.
(4) Garnier, J.; Osguthorpe, D. J.; Robson, B. *J. Mol. Biol.* **1978**, *120*, 97–120.
(5) Niemeyer, C. M. *Angew. Chem., Int. Ed.* **2001**, *40*, 4128–4158.
(6) Xu, Y.; Oyola, R.; Gai, F. *J. Am. Chem. Soc.* **2003**, *125*, 15388–15394.
(7) Tamm, L. K.; Tatulian, S. A. *Q. Rev. Biophys.* **1997**, *30*, 365–429.
(8) Byler, D. M.; Susi, H. *Biopolymers* **1986**, *25*, 469–487.
(9) Barth, A.; Zscherp, C. *Q. Rev. Biophys.* **2002**, *35*, 369–430.
(10) Zaitseva, E.; Saavedra, M.; Banerjee, S.; Sakmar, T. P.; Vogel, R. *Biophys. J.* **2010**, *99*, 2327–2335.
(11) Mendelsohn, R.; Brauner, J. W.; Gericke, A. *Annu. Rev. Phys. Chem.* **1995**, *46*, 305–334.
(12) Shim, S. H.; Strasfeld, D. B.; Ling, Y. L.; Zanni, M. T. *Proc. Natl. Acad. Sci. U.S.A.* **2007**, *104*, 14197–14202.
(13) Ganim, Z.; Chung, H. S.; Smith, A. W.; Deflores, L. P.; Jones, K. C.; Tokmakoff, A. *Acc. Chem. Res.* **2008**, *41*, 432–441.
(14) Maekawa, H.; Formaggio, F.; Toniolo, C.; Ge, N.-H. *J. Am. Chem. Soc.* **2008**, *130*, 6556–6566.
(15) Woys, A. M.; Lin, Y. S.; Reddy, A. S.; Xiong, W.; de Pablo, J. J.; Skinner, J. L.; Zanni, M. T. *J. Am. Chem. Soc.* **2010**, *132*, 2832–2838.
(16) Shen, Y. R. *Nature* **1989**, *337*, 519–525.
(17) Eisenthal, K. B. *Chem. Rev.* **1996**, *96*, 1343–1360.
(18) Richmond, G. L. *Chem. Rev.* **2002**, *102*, 2693–2724.
(19) Chen, Z.; Shen, Y. R.; Somorjai, G. A. *Annu. Rev. Phys. Chem.* **2002**, *53*, 437–465.
(20) Wang, H.-F.; Gan, W.; Lu, R.; Rao, Y.; Wu, B.-H. *Int. Rev. Phys. Chem.* **2005**, *24*, 191–256.
(21) Shultz, M. J.; Schnitzer, C.; Simonelli, D.; Baldelli, S. *Int. Rev. Phys. Chem.* **2000**, *19*, 123–153.
(22) Benderskii, A. V.; Henzie, J.; Basu, S.; Shang, X. M.; Eisenthal, K. B. *J. Phys. Chem. B* **2004**, *108*, 14017–14024.
(23) Su, X. C.; Cremer, P. S.; Shen, Y. R.; Somorjai, G. A. *J. Am. Chem. Soc.* **1997**, *119*, 3994–4000.
(24) Lu, G. Q.; Lagutchev, A.; Dlott, D. D.; Wieckowski, A. *Surf. Sci.* **2005**, *585*, 3–16.
(25) Liu, J.; Conboy, J. C. *J. Am. Chem. Soc.* **2004**, *126*, 8376–8377.
(26) Haupert, L. M.; Simpson, G. J. *Annu. Rev. Phys. Chem.* **2009**, *60*, 345–365.
(27) Walter, S. R.; Geiger, F. M. *J. Phys. Chem. Lett.* **2009**, *1*, 9–15.
(28) Wang, J.; Chen, X. Y.; Clarke, M. L.; Chen, Z. *Proc. Natl. Acad. Sci. U.S.A.* **2005**, *102*, 4978–4983.
(29) Nagahara, T.; Kisoda, K.; Harima, H.; Aida, M.; Ishibashi, T. *J. Phys. Chem. B* **2009**, *113*, 5098–5103.
(30) Fu, L.; Ma, G.; Yan, E. C. Y. *J. Am. Chem. Soc.* **2010**, *132*, 5405–5412.
(31) Lopes, D. H. J.; Meister, A.; Gohlke, A.; Hauser, A.; Blume, A.; Winter, R. *Biophys. J.* **2007**, *93*, 3132–3141.
(32) DeGrado, W. F.; Lear, J. D. *J. Am. Chem. Soc.* **1985**, *107*, 7684–7689.
(33) Andreev, O. A.; Karabadzhak, A. G.; Weerakkody, D.; Andreev, G. O.; Engelman, D. M.; Reshetnyak, Y. K. *Proc. Natl. Acad. Sci. U.S.A.* **2010**, *107*, 4081–4086.
(34) Palczewski, K.; Kumasaka, T.; Hori, T.; Behnke, C. A.; Motoshima, H.; Fox, B. A.; Le Trong, I.; Teller, D. C.; Okada, T.; Stenkamp, R. E.; Yamamoto, M.; Miyano, M. *Science* **2000**, *289*, 739–745.
(35) Mermut, O.; Phillips, D. C.; York, R. L.; McCrea, K. R.; Ward, R. S.; Somorjai, G. A. *J. Am. Chem. Soc.* **2006**, *128*, 3598–3607.
(36) Weidner, T.; Apte, J. S.; Gamble, L. J.; Castner, D. G. *Langmuir* **2009**, *26*, 3433–3440.
(37) Korenbrot, J. I.; Jones, O. *J. Membr. Biol.* **1979**, *46*, 239–254.
(38) Lavoie, H.; Desbat, B.; Vaknin, D.; Salesse, C. *Biochemistry* **2002**, *41*, 13424–13434.
(39) Westermark, P.; Engstrom, U.; Johnson, K. H.; Westermark, G. T.; Betsholtz, C. *Proc. Natl. Acad. Sci. U.S.A.* **1990**, *87*, 5036–5040.
(40) Liu, J.; Liu, M. Y.; Nguyen, J. B.; Bhagat, A.; Mooney, V.; Yan, E. C. Y. *J. Am. Chem. Soc.* **2009**, *131*, 8750–8751.
(41) Ma, G.; Liu, J.; Fu, L.; Yan, E. C. Y. *Appl. Spectrosc.* **2009**, *63*, 528–537.
(42) Chirgadze, Y. N.; Nevskaya, N. A. *Biopolymers* **1976**, *15*, 627–636.
(43) Reddy, A. S.; Wang, L.; Lin, Y.-S.; Ling, Y.; Chopra, M.; Zanni, M. T.; Skinner, J. L.; De Pablo, J. J. *Biophys. J.* 2010, *98*, 443–451.
(44) Shim, S. H.; Gupta, R.; Ling, Y. L.; Strasfeld, D. B.; Raleigh, D. P.; Zanni, M. T. *Proc. Natl. Acad. Sci. U.S.A.* **2009**, *106*, 6614–6619.
(45) Luca, S.; Yau, W.-M.; Leapman, R.; Tycko, R. *Biochemistry* **2007**, *46*, 13505–13522.
(46) Hoppener, J. W. M.; Ahren, B.; Lips, C. J. M. *New Engl. J. Med.* **2000**, *343*, 411–419.
(47) Hebda, J. A.; Miranker, A. D. *Annu. Rev. Biophys.* **2009**, *38*, 125–152.
(48) Petkova, A. T.; Leapman, R. D.; Guo, Z.; Yau, W.-M.; Mattson, M. P.; Tycko, R. *Science* **2005**, *307*, 262–265.
(49) Perry, J. M.; Moad, A. J.; Begue, N. J.; Wampler, R. D.; Simpson, G. J. *J. Phys. Chem. B* **2005**, *109*, 20009–20026.
(50) Wang, J. P. *Chem. Phys. Lett.* **2009**, *467*, 375–380.
(51) Belkin, M. A.; Shen, Y. R. *Int. Rev. Phys. Chem.* **2005**, *24*, 257–299.
(52) Nguyen, K. T.; King, J. T.; Chen, Z. *J. Phys. Chem. B* **2010**, *114*, 8291–8300.